

METABOLISM OF THE HIV-1 REVERSE TRANSCRIPTASE INHIBITOR DELAVIRDINE IN MICE

MAYLAND CHANG, VIRENDRA K. SOOD, GRACELLA J. WILSON, DAVID A. KLOOSTERMAN, PHILLIP E. SANDERS, MICHAEL J. HAUER, WEIRONG ZHANG, AND DANIEL G. BRANSTETTER

Drug Metabolism Research (M.C., V.K.S., G.J.W., P.E.S., M.J.H.); Structural, Analytical and Medicinal Chemistry (D.A.K.); and Investigative Toxicology (W.Z., D.G.B.), Pharmacia & Upjohn, Inc.

(Received December 2, 1996; accepted March 17, 1997)

ABSTRACT:

Delavirdine mesylate (U-90152T) is a highly specific nonnucleoside HIV-1 reverse transcriptase inhibitor currently under development for the treatment of AIDS. The excretion, disposition, brain penetration, and metabolism of delavirdine were investigated in CD-1 mice after oral administration of [^{14}C]delavirdine mesylate at single doses of 10 and/or 250 mg/kg and multiple doses of 200 mg/kg/day. Studies were conducted with ^{14}C -carboxamide and 2- ^{14}C -pyridine labels, as well as $^{13}\text{C}_3$ -labeled drug to facilitate metabolite identification. Excretion was dose dependent with 57–70% of the radioactivity eliminated in feces and 25–36% in urine. Pharmacokinetic analyses of delavirdine and its *N*-desisopropyl metabolite (desalkyl delavirdine) in plasma showed that delavirdine was absorbed and metabolized rapidly, that it constituted a minor component in circulation, that its pharmacokinetics were nonlinear,

and that its metabolism to desalkyl delavirdine was capacity limited or inhibitable. Delavirdine did not significantly cross the blood-brain barrier; however, its *N*-isopropylpyridinepiperazine metabolite—arising from amide bond cleavage—was present in brain at levels 2- to 3-fold higher than in plasma. The metabolism of delavirdine in the mouse was extensive and involved amide bond cleavage, *N*-desalkylation, hydroxylation at the C-6' position of the pyridine ring, and pyridine ring-cleavage as determined by MS and/or ^1H and ^{13}C NMR spectroscopies. *N*-desalkylation and amide bond cleavage were the primary metabolic pathways at low drug doses and, as the biotransformation of delavirdine to desalkyl delavirdine reached saturation or inhibition, amide bond cleavage became the predominant pathway at higher doses and after multiple doses.

Human immunodeficiency virus type 1 (HIV-1) infection resulting in AIDS is currently the leading cause of death in males 25 to 45 years of age in the United States (1). An important step in the replication of HIV-1 involves transcription of viral genomic RNA into proviral DNA by reverse transcriptase (2–4). Reverse transcriptase inhibitors such as 3'-azido-3'-eoxythymidine (AZT, zidovudine) (5, 6), 2',3'-dideoxyinosine (ddI, didanosine) (7–9), 2',3'-dideoxycytidine (ddC, zalcitabine) (10), 2',3'-dideoxy-3'-deoxythymidine (d4T, stavudine) (11), and (-)-2'-deoxy-3'-thiacytidine (3TC, lamivudine) (12, 13) are nucleoside prodrugs that are converted by cellular enzymes to the active deoxynucleotide triphosphates that lack a free 3'-hydroxyl group and lead to chain termination and inhibition of viral replication. However, the serious toxic side effects (14) resulting from inhibition of cellular DNA polymerases (6, 8, 14, 15) and the emergence of resistant strains of the virus (16–20) have focused efforts on the development of specific nonnucleoside reverse transcriptase inhibitors. A new potent and highly specific HIV-1 reverse transcriptase inhibitor, delavirdine mesylate (U-90152T, fig. 1), was discovered

¹ Abbreviations used are: HIV-1, human immunodeficiency virus type 1; IC₅₀, median inhibitory concentration; LSC, liquid scintillation counting; DMSO, dimethylsulfoxide; PB, particle beam; CI, chemical ionization; LC, liquid chromatography; MS, mass spectrometry; PCI, positive chemical ionization; EI, electron ionization; 2D, two-dimensional; DEPT, distortionless enhancement by polarization transfer; COSY, correlation spectroscopy; HMQC, heteronuclear multiple-quantum correlation; GARP, globally optimized alternating-phase rectangular pulses; HMBC, heteronuclear multiple-bond correlation.

Send reprint requests to: Dr. Mayland Chang, Drug Metabolism Research, Pharmacia & Upjohn, Inc., Kalamazoo, MI 49007.

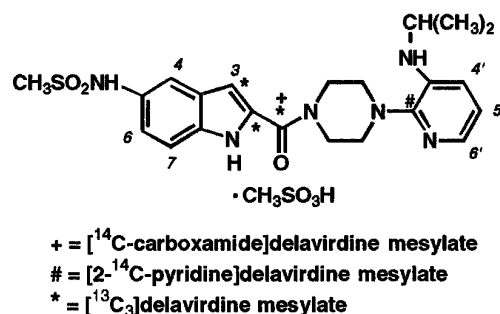


FIG. 1. Structure of delavirdine mesylate including the positions of the ^{14}C and ^{13}C labels.

recently (21, 22). Delavirdine selectively inhibited recombinant HIV-1 reverse transcriptase with an IC₅₀ of 0.26 μM (22) and blocked viral replication in peripheral blood lymphocytes of 25 primary HIV-1 isolates, including strains which were highly resistant to AZT or ddI, with a 50% effective concentration of 0.066 μM (22). The potent inhibition of replication by delavirdine was comparable to the antiviral activity of nucleoside or other nonnucleoside reverse transcriptase inhibitors (21, 22). Delavirdine exhibited no significant inhibition of cellular polymerases α and β with IC₅₀s of >440 μM (22). Delavirdine mesylate is currently under phase III clinical evaluations for the treatment of AIDS. This study describes the excretion, disposition, and brain penetration of delavirdine and its metabolites, and the isolation and identification of the metabolites of delavirdine after oral administration of [^{14}C]delavirdine mesylate to male and female CD-1

mice. Studies were conducted with ^{14}C -carboxamide and 2- ^{14}C -pyridine labels, as well as $^{13}\text{C}_3$ -labeled drug to facilitate metabolite identification.

Materials and Methods

Chemicals. All chemicals used in this study were of analytical grade. Solvents were Burdick & Jackson high purity grade (Burdick & Jackson, Muskegon, MI). Water was distilled and purified through a Milli-Q reagent water system (Millipore Corp., Bedford, MA). Ultima Gold (Packard Instruments, Meriden, CT) was used for liquid scintillation counting (LSC). Carbo-sorb E (Packard) and Permafluor E⁺ (Packard) were used for combustion of samples. Ultima-Flo M (Packard) was used as scintillant for flow-through detection. β -Glucuronidase (*Helix pomatia*, Type H-5) was obtained from Sigma Chemical Company (St. Louis, MO). Methanol- d_4 (99.96% D) and DMSO- d_6 were purchased from Cambridge Isotope Laboratories (Cambridge, MA).

Delavirdine mesylate, [^{14}C -carboxamide]delavirdine mesylate, [$^{13}\text{C}_3$]delavirdine mesylate, [2- ^{14}C -pyridine]delavirdine mesylate, U-96183, U-102466, U-88703, U-88822, U-96364, and U-91976 were synthesized by Pharmacia & Upjohn, Inc. The specific activities of the radiolabeled test substances were 57.8 $\mu\text{Ci}/\text{mg}$ for [^{14}C -carboxamide]delavirdine mesylate and 79.58 $\mu\text{Ci}/\text{mg}$ for [2- ^{14}C -pyridine]delavirdine mesylate, with radiochemical purities of >99% by HPLC. The chemical purities of the nonradiolabeled and [$^{13}\text{C}_3$]delavirdine mesylate were >97.7% and 97.7%, respectively. The structure and positions of the ^{14}C and ^{13}C labels are shown in fig. 1.

Animals. CD-1 mice were obtained from Charles River Laboratories (Portage, MI). Male mice weighed 23–37 g and were 6–7 weeks old at dose administration. Female mice weighed 17–29 g and were 7–8 weeks old. For excretion studies, mice were placed in individual Nalgene metabolism cages equipped with urine and feces separators. Mice used for collection of blood samples and in the brain penetration study were housed in individual stainless steel cages with wire mesh floors. Environmental conditions were maintained as follows: lights 12 hr on/12 hr off, relative humidity 41–64%, temperature 68–75°F, ventilation 18–20 room air changes per hr. Mice were provided with food (Certified Rodent Diet 5002M or 5002C, or Certified Mouse Diet 5015, PMI Feeds Inc., St Louis, MO) and water *ad libitum*. Mice were fasted approximately 3 hr before and 1 hr after radiolabeled dose administration. The animals in this study were cared for and used in accordance with *The Guide for the Care and Use of Laboratory Animals*, DHEW Publication (National Institutes of Health) 85–23, 1985 and with *The Animal Welfare Act Regulation 9 CFR 3*, August 15, 1989 and as modified on March 19, 1991.

Instrumentation. Samples were oxidized in a Packard Model 307 sample oxidizer (Packard Instrument Co., Meriden, CT) equipped with a Packard Oximate 80 robotics system. A Packard Tri-Carb Liquid Scintillation Analyzer Model 1900 CA or Model 1900TR was used for radioactivity counting. Feces were homogenized using a Stomacher Blender (Tekmar Co., Cincinnati, OH). A TurboVap LV evaporator (Zymark Corporation, Hopkinton, MA) or a SpeedVac concentrator Model SVC 100H (Savant Instruments, Inc., Farmingdale, NY) was used to concentrate samples.

Chromatography. The HPLC system consisted of a Perkin Elmer Series 410 quaternary pump (Perkin-Elmer Corp., Norwalk, CT), a Perkin Elmer ISS 200 LC sample processor, a Perkin Elmer LC-235C diode array detector, and a Radiomatic Model A-515 or A-525 flow-through detector (Packard Instrument Co., Meriden, CT) containing a 500- μl liquid cell. HPLC columns and guard cartridges were obtained from YMC, Inc. (Wilmington, NC) or MacMod Analytical Inc. (Chadds Ford, PA). A Foxy 200 fraction collector (Isco, Inc., Lincoln, NE) equipped with a diverter valve was used to collect fractions at 0.5-min intervals on a recycling mode.

Mass Spectrometry. PB-LC-MS was performed using a Finnigan 4021 quadrupole (Finnigan MAT, San Jose, CA) or a VG Autospec Q hybrid (Fisons, Manchester, UK) mass spectrometer equipped with a particle beam interface (Thermabeam, Extrel Corporation, Pittsburgh, PA; interface built at Pharmacia & Upjohn, Inc.). The instrument was operated in PCI mode using ammonia as reagent gas or in EI mode. Electron energy was set at 70 eV. HPLC analyses were performed on a system consisting of a Perkin Elmer ISS 100 sample processor interfaced to a Perkin Elmer Series 410 quaternary pump with a Perkin Elmer SEC-4 solvent environment control and a Waters 490MS

UV detector (Waters, Milford, MA). The mobile phase consisted of elution on a with a YMC 5 μ -basic 4.6 mm i.d. \times 25 cm column at 0.5 ml/min with a 20-min linear gradient from 10% A/90% D to 60% A/40% D, followed by 20-min 60% A/40% D, then a 10-min linear gradient to 80% A/20% D; where A = acetonitrile, D = 0.1 M ammonium acetate (pH 4). Alternatively, samples were isocratically eluted at 0.5 ml/min with 35% acetonitrile/2% isopropyl alcohol/63% 0.1 M ammonium acetate (pH 4).

Electrospray ionization-mass spectrometry (ESI-MS) was performed on a Finnigan-MAT TSQ 7000 triple quadrupole mass spectrometer (Finnigan-MAT, San Jose, CA) directly coupled to the HPLC system *via* a Finnigan atmospheric pressure ionization (API) source operated in the ESI mode. The HPLC system consisted of a Hewlett Packard 1050 Series pump and autosampler (Hewlett Packard, Naperville, FL), and a Thar two position valve actuator (Thar Designs Inc., Pittsburgh, PA). The mobile phase was the same as for PB-LC-MS, except for a flow rate of 1.0 ml/min. Flow to the mass spectrometer was split 1:2.

Nuclear Magnetic Resonance Spectroscopy. ^1H NMR spectra were recorded at 500 MHz using a Bruker AMX-500 spectrometer (Bruker Instruments Inc., Billerica, MA). Data were processed on a Bruker X-32 computer using Bruker UXNMR software version 930901.3. Samples were dissolved in approximately 300–500 μl methanol- d_4 in a 3 mm i.d. Teflon insert (WILMAD, Buena, NJ); the Teflon insert was placed in a 5 mm NMR tube (WILMAD). Spectra were recorded at a temperature of 300°K as free induction decays of 32K complex points. The residual CHD₂OH pentet was used as reference at 3.30 ppm.

2D ^1H COSY spectra were recorded in the magnitude mode using 1K by 1K data table with 256 increments in F1 and no zero-filling in F2. Unshifted sinebell windows were applied before transformation.

2D inverse ^1H - ^{13}C HMQC spectra (23) were recorded in the magnitude mode with a relaxation delay of 0.8 sec, GARP decoupling of ^{13}C during acquisition (24), a 1K by 512W data table, and 128 increments in F1 with no zero-filling in F2. Sinebell-squared window functions shifted $\pi/2$ radians were applied in both F2 and F1.

2D inverse ^1H - ^{13}C HMQC spectra (25) were recorded using the same conditions described for the HMQC spectra except that a relaxation delay of 1.0 sec was used with no ^{13}C decoupling. The low-pass J-filter was optimized for 6 Hz to suppress crosspeaks arising from ^1H - ^{13}C one-bond correlations.

^{13}C NMR spectra were recorded at 125.75 MHz using a Bruker AMX-500 spectrometer. One-dimensional ^{13}C and ^{13}C - ^1H DEPT (26) spectra were recorded as free induction decays of 32K complex points, using a 30° ^{13}C pulse and a repetition rate of approximately 1 sec with proton decoupling. The free induction decay was zero-filled once, multiplied by a slightly line-broadening (LB = 1 Hz) decaying exponential function, and Fourier transformed. Methanol- d_4 was used as reference at 49.0 ppm.

Ultraviolet Spectrometry. UV spectra were obtained on a Perkin Elmer LC-235C diode array detector as described previously (27).

Dosing and Sample Collection. Doses were measured gravimetrically and administered by oral gavage using a dosing syringe attached to an animal feeding needle. Blood samples were stored on ice and centrifuged to separate the plasma. Urine, feces, and tissue samples were collected at room temperature, immediately analyzed, or stored at -20°C until further analysis.

Single-Dose Excretion and Metabolism [^{14}C -Carboxamide]Delavirdine Mesylate Study. Delavirdine mesylate and [^{14}C -carboxamide]delavirdine mesylate were dissolved in 80% propylene glycol/20% water containing 3 μl methanesulfonic acid per ml to final concentrations of 2 and 50 mg/ml. Thirty-one male and 31 female mice received single oral doses of approximately 10 mg/kg and 585 $\mu\text{Ci}/\text{kg}$, and 31 male and 31 female mice were administered single oral doses of approximately 250 mg/kg and 595 $\mu\text{Ci}/\text{kg}$. Urine was collected from 4 mice/sex/dose over 0–12, 12–24, and at 24-hr intervals up to 120 hr post-dose; feces were collected over 0–24 and at 24-hr intervals up to 120 hr after dosing. Terminal blood samples were collected by cardiac puncture from the remaining mice (3 mice/sex/dose/time point) at scheduled times through the 48-hr period following the radiolabeled dose.

Multiple-Dose Excretion and Metabolism [$^{13}\text{C}_3$, ^{14}C -Carboxamide]Delavirdine Mesylate Study. Equimolar amounts of delavirdine mesylate and [$^{13}\text{C}_3$]delavirdine mesylate were mixed with [^{14}C -carboxamide]delavirdine mesylate and dissolved in 80% propylene glycol/20% water containing 3 μl methanesulfonic acid per ml to a final concentration of 20 mg/ml. Three male

mice received multiple oral radiolabeled doses of 200 mg/kg/day and 272 $\mu\text{Ci}/\text{kg}/\text{day}$. Doses were given twice a day, one dose in the morning and a second dose 8 hr later for 4.5 days. Urine and feces were collected at 24-hr intervals up to 216 hr after the first dose. A terminal blood sample was collected from one mouse by cardiac puncture 4 hr after the last dose; urine and feces from this mouse were collected at 24-hr intervals up to 96 hr after the first dose.

Single-Dose Excretion and Metabolism [2- ^{14}C -Pyridine]Delavirdine Mesylate Study. Delavirdine mesylate and [2- ^{14}C -pyridine]delavirdine mesylate were dissolved in 80% propylene glycol/20% water containing 3 μl methanesulfonic acid per ml to a final concentration of 50 mg/ml. Six male mice were administered single oral doses of approximately 250 mg/kg and 1,200 $\mu\text{Ci}/\text{kg}$. Terminal blood was collected from 3 mice at 0.5, 1, and 2 hr after dosing. Urine and feces were collected from the remaining 3 mice; urine over the time periods 0–12, 12–24, 24–48, and 48–72 hr after dosing, and feces at 24-hr intervals to 72 hr post-dose.

Single-Dose Brain Penetration [2- ^{14}C -Pyridine]Delavirdine Mesylate Study. Delavirdine mesylate and [2- ^{14}C -pyridine]delavirdine mesylate were dissolved in 50% propylene glycol/50% water containing 3 μl methanesulfonic acid per ml to a final concentration of 50 mg/ml. Twelve female mice were administered single oral doses of approximately 250 mg/kg and 975 $\mu\text{Ci}/\text{kg}$. Terminal blood and excised unperfused tissues (brain and pituitary) were collected at 1, 4, 12, and 24 hr after dosing.

Sample Preparation and Total Radiocarbon Analysis. Aliquots of urine (3 replicates) and plasma (1–2 replicates) were analyzed by LSC. Whole blood (2 replicates), feces (3–5 replicates), and brain (3 replicates) were combusted prior to LSC analysis. Feces and brain were homogenized with 3–5 volumes of water with and without 2% acetic acid, respectively.

The combustion efficiency of the sample oxidizer was determined by comparing the radioactivity recovered from replicate oxidations of pre-dose feces, whole blood, or tissue fortified with a known amount of [^{14}C -carboxamide] or [2- ^{14}C -pyridine]delavirdine mesylate to that obtained by direct fortification of the Carbo-sorb/Permafluor trapping solution with the

same amount of [^{14}C]delavirdine mesylate. The efficiency was calculated at the start of a series of oxidations, as well as intermittently, to ensure that the oxidizer efficiency did not change substantially; concentrations were corrected for combustion efficiency. Radioactivity was measured by LSC with 2–20 min counting. Count rates in cpm were corrected to dpm using quench curves generated from sealed quenched standards in either Ultima Gold or Carbo-sorb/Permafluor cocktails.

HPLC Analyses of Plasma for Delavirdine and Desalkyl Delavirdine. Plasma samples from the single-dose excretion and metabolism [^{14}C -carboxamide]delavirdine mesylate study were analyzed for delavirdine and desalkyl delavirdine as follows: A 25- μl aliquot of plasma was mixed with 75 μl internal standard solution in acetonitrile (1 $\mu\text{g}/\text{ml}$ U-88822 in acetonitrile) and centrifuged at 14,000 rpm for 5 min at 4°C. A 90- μl aliquot of the supernatant was evaporated to dryness and reconstituted in 200 μl of 10% acetonitrile/90% 0.1 M ammonium acetate buffer (pH 4), and a 100- μl portion was analyzed by HPLC with UV detection at 295 nm. The HPLC conditions consisted of isocratic elution on a YMC 5 μ -basic 4.6 mm i.d. \times 25 cm column at a flow of 1.0 ml/min with 34% acetonitrile/2% isopropyl alcohol/64% 0.1 M ammonium acetate buffer (pH 4). Quantitation of delavirdine and desalkyl delavirdine in plasma was determined using peak area ratios relative to the internal standard and linear regression parameters calculated from calibration curve standards. Calibration curve and quality control standards were prepared similarly in blank mouse plasma.

Pharmacokinetic Analysis. Pharmacokinetic parameter estimates were determined by noncompartmental analyses of the dose-normalized mean concentration-time data for drug-related material, delavirdine, and desalkyl delavirdine. AUC was determined by the linear trapezoidal rule. Half-lives were estimated from the terminal linear portion of the dose-normalized mean concentration-time data by linear regression, where the slope of the line was the rate constant k and $t_{1/2} = \ln 2/k$. t_{max} was the time at which maximum concentration (C_{max}) was achieved; both values were based on the highest observed concentrations.

HPLC Profiles of Plasma, Urine, Feces, and Brain Samples. Plasma,

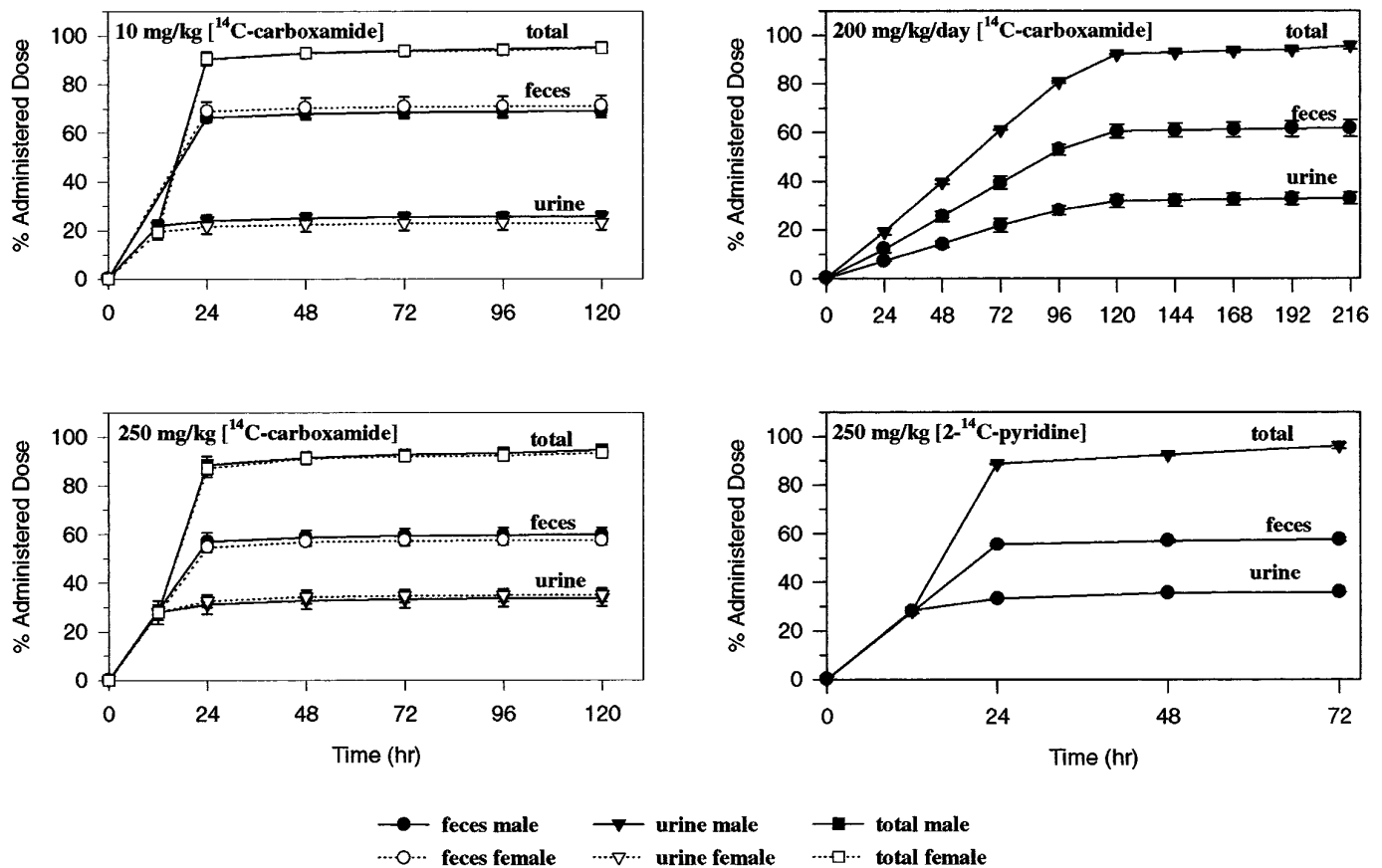


FIG. 2. Excretion of drug-related radioactivity in mice after single and multiple oral dose administration of [^{14}C -carboxamide]delavirdine mesylate.

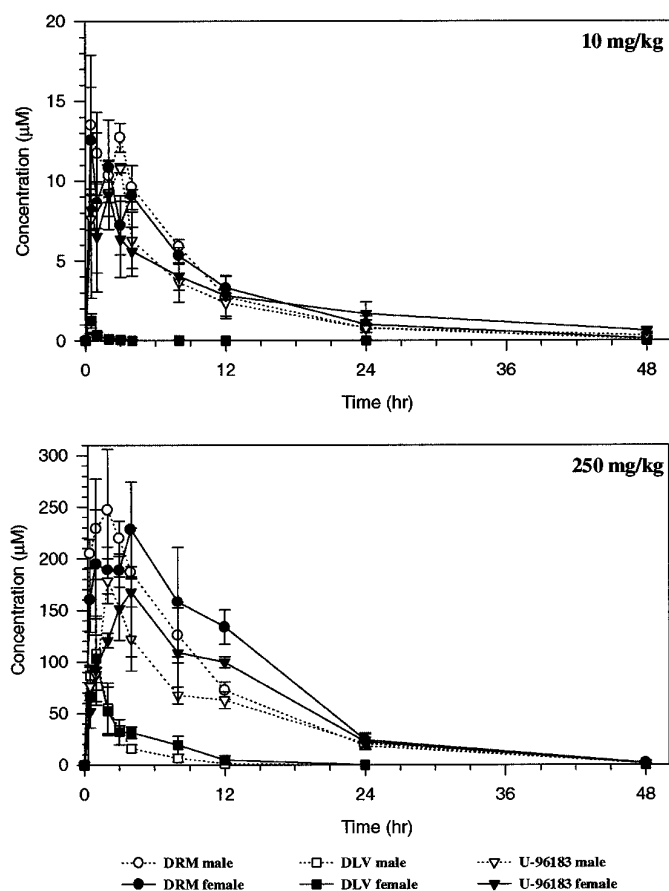


FIG. 3. Plasma concentration-time profiles of drug-related material, delavirdine, and desalkyl delavirdine in mice after single oral dose administration of [^{14}C -carboxamide]delavirdine mesylate.

urine, feces, and brain samples were profiled for parent drug and metabolites by HPLC with flow-through radiochemical detection. Urine samples were directly profiled; plasma samples were deproteinated by precipitation with acetonitrile. Feces (2- to 8-g aliquots) samples were extracted with 90% acetonitrile/10% 0.1 M ammonium acetate (pH 4) or 70% methanol/30% water containing 2% acetic acid and concentrated prior to HPLC analysis. The extraction recoveries of radioactivity were $76.0 \pm 2.2\%$ for feces from the multiple-dose excretion and metabolism [$^{13}\text{C}_3$, ^{14}C -carboxamide]delavirdine mesylate study and $55.4 \pm 0.4\%$ for feces from the single-dose excretion and metabolism [$^{13}\text{C}_3$, ^{14}C -pyridine]delavirdine mesylate study. Brain samples (1.7 g) were extracted with acetone ($96 \pm 2\%$) and concentrated prior to HPLC analysis. Extraction procedures were validated with pre-dose fecal and brain homogenate fortified with [^{14}C -carboxamide] and/or [^{14}C -pyridine]delavirdine mesylate (recoveries of approximately 98% for feces and 101.5% for brain). Chromatographic analyses were performed on a YMC 5μ -basic 4.6 mm i.d. \times 25 cm column using gradient elution at 1.0 ml/min with 10% A/90% D for 5 min, followed by a 35-min linear gradient to 60% A/40% D, then 60% A/40% D for 5 min (where A = acetonitrile, D = 0.1 M ammonium acetate buffer (pH 4)). The HPLC effluent was mixed with Ultima-Flo M in a 1:3 ratio. Peaks of radioactivity were quantified on the Radiomatic detector using peak area integration. Column recovery was determined by comparing the total radioactivity from the sum of the integrated peaks in the ^{14}C chromatogram with total radioactivity; essentially all of the injected radioactivity was recovered from the column.

Metabolite Isolation. MET-10 was isolated as follows: Urine (48 ml, 12.66×10^6 dpm, 4.2 mg of drug-related material) collected over the time period 0–24 hr from three mice in the multiple-dose excretion and metabolism [$^{13}\text{C}_3$, ^{14}C -carboxamide]delavirdine mesylate study was lyophilized. The resi-

TABLE 1
Mean \pm SD pharmacokinetic parameters^a for drug-related material, delavirdine, and desalkyl delavirdine after single oral dose administration of [^{14}C -carboxamide]delavirdine mesylate

Dose (mg/kg)	Sex/N	Analyte ^b	AUC ^c ($\mu\text{M}/\text{hr}$)	C_{max} (μM)	t_{max} (hr)	$t_{1/2}$ (hr)
10	M/3	DRM	123	13.5 ± 4.4	0.5	7.3
		DLV	1.01	0.81 ± 0.40	0.5	0.81
		Desalkyl DLV	97.5	10.8 ± 0.3	3.0	7.4
10	F/3	DRM	120	12.5 ± 3.3	0.5	7.2
		DLV	1.01	1.25 ± 0.45	0.5	0.84
		Desalkyl DLV	115	9.15 ± 2.16	2.0	8.0
250	M/3	DRM	2640	247 ± 60	2.0	6.5
		DLV	288	108 ± 35	1.0	1.9
		Desalkyl DLV	1920	178 ± 22	2.0	8.8
250	F/3	DRM	3330	228 ± 45	4.0	5.7
		DLV	389	103 ± 42	1.0	3.2
		Desalkyl DLV	2440	168 ± 63	4.0	6.6

^a Pharmacokinetic parameters were determined from dose normalized mean concentrations. Pharmacokinetic parameters for individual mice and SD for mean data could not be calculated since only one blood draw per mouse could be obtained.

^b DRM, drug-related material; DLV, delavirdine.

^c AUC_(0–48) for DRM, DLV, and desalkyl DLV.

due was dissolved in 4.8 ml 10% acetonitrile/90% 0.1 M ammonium acetate (pH 4) to afford 12.3×10^6 dpm, 4.1 mg of drug-related material. A portion of the concentrated urine (10.5×10^6 dpm, 3.5 mg drug-related material) was purified by HPLC with gradient elution (YMC 5μ -basic 4.6 mm i.d. \times 25 cm, 21 injections of 200 μl each, 1.0 ml/min, 5-min 10% A/90% D, 35-min linear gradient to 60% A/40% D, 5-min 60% A/40% D, where A = acetonitrile, D = 0.1 M ammonium acetate buffer (pH 4)) to give 1.2 mg (3.6×10^6 dpm) of partially purified MET-10. A final HPLC purification with isocratic elution (Zorbax 5μ -SB-CN 4.6 mm i.d. \times 25 cm, 11 injections of 100 μl each, 1.0 ml/min, 10% acetonitrile/90% 0.1 M ammonium acetate buffer (pH 4)) afforded 1.0 mg (3.0×10^6 dpm) of purified MET-10.

Metabolite Identification. Concentrated plasma (2 hr post-dose from four male mice given 250 mg/kg single doses of [^{14}C -carboxamide]delavirdine mesylate) and urine (48–72 hr from the multiple-dose excretion and metabolism [$^{13}\text{C}_3$, ^{14}C -carboxamide]delavirdine mesylate and 0–12 hr from the single-dose excretion and metabolism [^{14}C -pyridine]delavirdine mesylate study) were analyzed by EI and PCI-PB-LC-MS.

The purified MET-10 was dissolved in ~ 400 μl methanol- d_4 and analyzed by one-dimensional ^1H NMR, 2D COSY NMR, 2D HMQC NMR, and 2D HMBC NMR. A 50- μl portion of MET-10 in methanol- d_4 was diluted with 50 μl water for EI-PB-MS analysis.

Enzyme Hydrolysis. Plasma (deproteinated and concentrated samples 0.5 hr post-dose from 3 male mice given 10 mg/kg in the single-dose excretion and metabolism [^{14}C -carboxamide]delavirdine mesylate study) and 1 hr post-dose from a male mouse in the single-dose excretion and metabolism [^{14}C -pyridine]delavirdine mesylate study) and urine (0–12 hr from one mouse in the single-dose excretion and metabolism [^{14}C -pyridine]delavirdine mesylate study) were mixed (1:1) with 0.1 M sodium acetate (pH 5) and 200 μl β -glucuronidase solution (500 units/ml in 0.2% saline), followed by incubation at 37°C for 1 hr. Samples were analyzed by HPLC with flow-through radiochemical detection using gradient elution (*vide supra*). Control plasma and urine samples were prepared in 0.1 M sodium acetate (pH 5) and 200 μl 0.2% saline, followed by incubation at 37°C for 1 hr.

Acid Hydrolysis. Plasma supernatant (from the 10 mg/kg single-dose excretion and metabolism [^{14}C -carboxamide]delavirdine mesylate and single-

TABLE 2
Excretion of delavirdine and its metabolites after single and multiple oral dose administration of [¹⁴C]delavirdine mesylate^a

Dose mg/ kg/day	Sex/N	Dose Freq.	Matrix	¹⁴ C-carboxamide]Delavirdine Mesylate									
				MET-2 Despyridinyl DLV	MET-9 ^b Indole Carboxylic Acid conj.	MET-10 Indole Carboxylic Acid	MET-3 ^c Desalkyl DLV conjugate	MET-4a N-Sulf Desalkyl DLV	MET-5 Desalkyl DLV	MET-6 6'- Ogluc DLV	MET-7 6'- OH DLV	DLV	
10	M/4	Single dose	Urine	1.8 ± 0.2	ND	8.2 ± 2.3	1.6 ± 1.1	0.5 ± 0.3	9.4 ± 0.4	0.3 ± 0.4	0.3 ± 0.4	ND	
	F/4			2.4 ± 0.5	ND	7.8 ± 2.1	1.3 ± 0.9	ND	9.4 ± 0.2	0.3 ± 0.6	ND	ND	
250	M/4	Single dose	Urine	1.6 ± 0.2	ND	14.8 ± 2.4	1.5 ± 0.9	0.1 ± 0.1	11.1 ± 3.0	0.4 ± 0.1	0.4 ± 0.1	ND	
	F/4			1.9 ± 0.2	ND	15.0 ± 2.6	2.4 ± 1.3	ND	11.4 ± 0.6	1.2 ± 0.1	ND	ND	
200	M/2	Multiple dose	Urine	1.3 ± 0.3	5.5 ± 3.1	11.4 ± 0.4	0.3 ± 0.1	ND	8.9 ± 1.0	0.1 ± 0.1	0.1 ± 0.1	ND	
			Feces	24.0 ± 0.4	ND	3.1 ± 0.7	2.3 ± 0.2	0.3 ± 0.0	7.9 ± 0.2	2.2 ± 0.1	2.2 ± 0.1	3.1 ± 0.6	
			Total	25.4 ± 0.7	5.5 ± 3.1	14.4 ± 1.1	2.6 ± 0.3	0.3 ± 0.0	16.8 ± 1.2	1.0 ± 0.2	2.3 ± 0.2	3.1 ± 0.6	

Dose mg/ kg/day	Sex/N	Dose Freq.	Matrix	¹⁴ C-Pyridine]Delavirdine Mesylate									
				MET-13 Desalkyl Pyridine Piperazine	MET-14 Pyridine Ring Opened	MET-12 N- IsoPr Pyridine Piperazine	MET-3 ^c Desalkyl DLV Conjugate	MET-4a N-Sulf Desalkyl DLV	MET-5 Desalkyl DLV	MET-6 6'- Ogluc DLV	MET-7 6'- OH DLV	DLV	
250	M/2	Single-dose	Urine	5.0 ± 1.5	1.1 ± 0.2	13.0 ± 3.5	4.6 ± 1.2	ND	9.9 ± 0.3	0.7 ± 0.3	ND	ND	
			Feces	ND	ND	0.8 ± 1.1	1.3 ± 0.0	ND	8.3 ± 1.1	ND	3.3 ± 0.3	25.9 ± 2.0	
			Total	5.0 ± 1.5	1.1 ± 0.2	13.7 ± 4.6	5.8 ± 1.3	ND	18.2 ± 0.8	0.7 ± 0.3	3.3 ± 0.3	25.9 ± 2.0	

^a Mean ± SD in percent of administered dose; values for feces were corrected for extraction recovery. Other minor metabolites are not listed. ND, not detected.

^b MET-9 was tentatively characterized as a labile conjugate of the indole carboxylic acid metabolite (U-96364).

^c MET-3 was tentatively characterized as a thermally labile conjugate of desalkyl delavirdine (U-96183).

dose excretion and metabolism [2-¹⁴C-pyridine]delavirdine mesylate studies) and urine (0–12 hr from one male mouse in the single-dose excretion and metabolism [2-¹⁴C-pyridine]delavirdine mesylate study) were mixed (1:1) with 1 N HCl, followed by incubation at 88°C for 1 hr. After cooling, a 100- μ l aliquot was analyzed by HPLC with flow-through radiochemical detection using gradient elution (*vide supra*). Control plasma and urine samples in 200 μ l 10% acetonitrile/90% 0.1 M ammonium acetate (pH 4) were carried out similarly.

Results

Mass Balance. The cumulative excretion of drug-related radioactivity following single and multiple oral dose administration of [¹⁴C-carboxamide]delavirdine mesylate and after single oral dose administration of [2-¹⁴C-pyridine]delavirdine mesylate is shown in fig. 2. Mean recoveries were 57–70% in feces, 25–36% in urine, for total recoveries (including cagewash) of 94–96%. Most of the dose (>87%) was excreted within 24 hr after dosing.

Plasma Concentrations and Pharmacokinetics. Absorption was rapid as evidenced by mean t_{max} values for drug-related material, delavirdine, and desalkyl delavirdine, which ranged from 0.5 to 4.0 hr (fig. 3, table 1). Mean AUC of drug-related material and desalkyl delavirdine increased proportionately with dose; however, mean AUC of delavirdine increased more than proportionately with drug dose. Concentrations of desalkyl delavirdine were significantly higher than delavirdine concentrations.

Desalkyl delavirdine was the major (72.5–81.9%) radioactive component in circulation after single doses of both [¹⁴C-carboxamide]delavirdine mesylate and [2-¹⁴C-pyridine]delavirdine mesylate. Delavirdine was also observed in circulation, ranging from 0.9% to 18.2%. The remaining radioactivity in plasma was associated with MET-3 (6.1–17.7%), MET-6 (0.2–2.2%), and MET-10 (0.3–0.9%) or MET-12 (1.1%). Gender-related differences in metabolite profiles were not observed.

Distribution of Delavirdine and its Metabolites into Brain Tissue. Concentrations of drug-related material in brain and pituitary reached a maximum 1 hr after drug administration and were $7.2 \pm 0.7\%$ and $168 \pm 18\%$ of corresponding levels in plasma, respectively. HPLC analyses of plasma and brain showed that the *N*-isopropylpyridinepiperazine metabolite constituted 1.1% and 72% of the radioactivity in plasma and brain, respectively. Brain concentrations of the *N*-isopropylpyridinepiperazine metabolite were 2- to 3-fold higher than those observed in plasma. In contrast, delavirdine concentrations in brain were 2.7% of plasma 1 hr after drug administration.

HPLC Profiles of Urine and Feces. The metabolism of delavirdine was extensive in the mouse, with a small amount of the administered dose excreted as intact drug (<3% of the dose, table 2) following single or multiple doses of [¹⁴C-carboxamide]delavirdine mesylate. At low single doses of the [¹⁴C-carboxamide] labeled drug, the major components in urine were MET-5 and MET-10, with MET-5 present in slightly higher levels than MET-10. At high single doses and following multiple doses of [¹⁴C-carboxamide]delavirdine mesylate, MET-10 was the major component in urine, while MET-5 was present in lower amounts. With the [2-¹⁴C-pyridine] label, MET-12 was the major component in urine and MET-5 was present in lower levels. Several minor metabolites were also observed in urine; MET-9 was only observed following multiple doses. Feces contained mostly MET-2 after multiple doses of [¹⁴C-carboxamide]delavirdine mesylate, and mostly intact drug after a 250 mg/kg single-dose of [2-¹⁴C-pyridine]delavirdine mesylate. Representative chromatograms are shown in fig. 4.

MET-2, MET-5, MET-12, MET-13, and Delavirdine. The presence of despyridinyl delavirdine (MET-2), desalkyl delavirdine

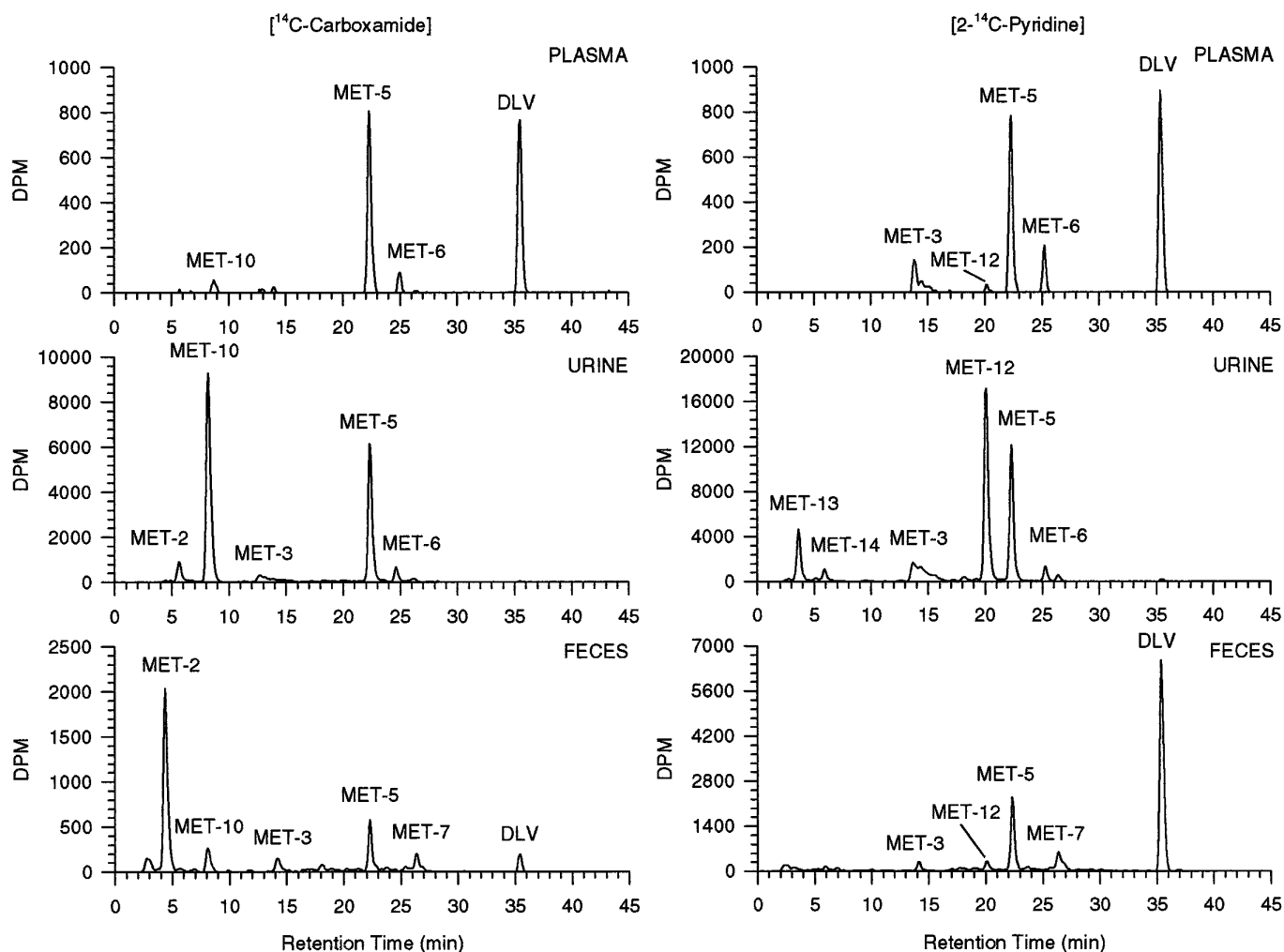


FIG. 4. Representative HPLC radiochromatograms of mouse plasma, urine, and feces after single oral dose administration of [^{14}C]delavirdine mesylate. Left top to bottom: plasma, urine, and feces [^{14}C -carboxamide] label; right top to bottom: plasma, urine, and feces [^{14}C -pyridine] label.

(MET-5), the *N*-isopropylpyridinepiperazine metabolite (MET-12), *N*-desisopropylpyridinepiperazine (MET-13), and delavirdine in urine and/or plasma was indicated by HPLC retention time and UV spectrum comparisons to synthetic standards. Structures were confirmed by comparison of the mass spectra of the metabolites (table 3, fig. 5) with those of synthetic standards.

MET-3. This minor component in plasma and urine was tentatively characterized as a thermally-labile conjugate of desalkyl delavirdine based on time-course profiles and enzyme and acid hydrolyses.

MET-1 and MET-4a. These minor metabolites in urine and feces were characterized as a conjugate and the sulfate conjugate of despyridinyl delavirdine, respectively, based on retention time comparison to MET-1 from rat feces (27) and MET-4a from dog urine (28).

MET-14. MET-14 was observed as a minor radioactive peak in urine after administration of [^{2-14}C -pyridine]delavirdine mesylate, but was not present after treatment with [^{14}C -carboxamide]delavirdine mesylate (fig. 4) and suggested that the structure of MET-14 lacked the carboxamide carbon. MET-14 in mice was characterized as the pyridine ring-opened metabolite based on HPLC retention time comparison with MET-14 isolated from rat feces and identified by ^1H NMR and MS-MS (27).

MET-6 and MET-7. These minor metabolites were observed in

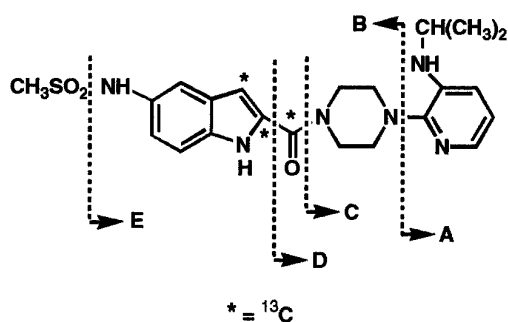
plasma and urine. Treatment of plasma and urine with β -glucuronidase (containing glucuronidase and sulfatase activities) or with acid resulted in the disappearance of MET-6 concomitant with an increase in MET-7. On further standing at room temperature, MET-7 degraded to despyridinyl delavirdine (MET-2) and to the pyridine ring-opened MET-14. These data suggested that MET-6 was a glucuronide or sulfate conjugate of MET-7.

Confirmation of MET-6 as a glucuronide was pursued by LC-MS analysis. However, because of the minor presence of this metabolite in mouse urine spectroscopic confirmation could not be obtained. MET-6 was characterized as 6'-*O*-glucuronide delavirdine based on HPLC retention time comparison with MET-6 isolated from rat bile and identified by ^1H NMR and MS (27).

Confirmation of MET-7 as 6'-hydroxy delavirdine was obtained by LC-MS. Analysis of urine from a mouse given [$^{13}\text{C}_3,^{14}\text{C}$ -carboxamide]delavirdine mesylate by CI-MS showed protonated molecular ions at m/z 473 and 476 (table 3), 16 amu higher than parent drug and indicative of the presence of a hydroxyl group. Cleavage of the pyridine-piperazine linkage gave ions at m/z 323 and 326, as well as an ion at m/z 153. The ion at m/z 153 was 16 amu higher than the corresponding ion for parent drug and established substitution on the pyridine ring. These data, together with the fact that enzyme hydro-

TABLE 3

Summary of key mass spectrometry fragmentation for delavirdine and its metabolites



Compound	Matrix	Ionization ^a Mode	MH ⁺ or M ⁺	Fragments (m/z) ^b				
				A	B	C	D	E
DLV	Plasma	EI	456	136	—	220	248	378
DLV ^c	Urine	CI, ESI	457, 460	137 ^d	—	—	—	—
MET-2 ^c	Urine	CI	323, 326	—	—	87	—	—
MET-5 ^c	Urine	CI, ESI	415, 418	—	323, 326 ^d	179	207, 208 ^d	337, 340 ^d
MET-5	Urine	CI	415	95	323	179	207	337
MET-5	Plasma	EI	414	93	321	178	—	336
MET-7 ^c	Urine	CI	473, 476	153	323, 326	—	—	—
MET-10 ^c	Urine	EI	254, 257	—	—	—	—	175, 178
MET-12	Urine	CI, ESI	221	137 ^d	—	—	—	—
MET-13	Urine	CI	179	—	—	—	—	—

^a CI, chemical ionization; EI, electron ionization; ESI, electrospray ionization.

^b Some fragments are not observed due to the structure of the compound or because of low concentrations.

^c Doublets 3 amu apart due to the presence of fragments containing ¹³C₃; fragments containing two or one ¹³C carbons gave doublets 2 or 1 amu apart, respectively; fragments with no ¹³C atoms gave singlets.

^d Not observed by ESI.

lysis of 6'-O-glucuronide delavirdine (MET-6) generated MET-7, identified MET-7 as 6'-hydroxy delavirdine.

MET-10. MET-10 was observed in mice treated with [¹⁴C-carboxamide]delavirdine mesylate, but not in mice given and [2-¹⁴C-pyridine]delavirdine mesylate. This metabolite eluted at the same HPLC retention time as the synthetic standard U-96364 (indole carboxylic acid metabolite). Confirmation of MET-10 was initially pursued by LC-MS. However, no spectroscopic information could be obtained because of the insensitivity of the technique for this metabolite. Therefore, MET-10 was isolated from mouse urine. MET-10 showed a UV λ_{max} at 293 nm, characteristic of the presence of an indole ring. The ¹H NMR spectrum (500 MHz, methanol-d₄, fig. 6, table 4) showed the presence of four aromatic protons and a methylsulfonamido group. Resonances for the pyridine and piperazine rings, as well as those for the isopropyl side chain were not observed. All four aromatic protons were similar to corresponding resonances in the parent drug (fig. 6, table 4) and were assigned to protons on the indole ring. The resonances at 6.74 and 7.09 ppm corresponded to H-3 split into two doublets owing to ²J_{CH} coupling of 7.5 Hz between C-2 and H-3 and ¹J_{CH} coupling of 175 Hz between C-3 and H-3. Therefore, the singlet at 6.91 ppm integrating for 0.6 protons corresponded to H-3 in the unenriched (99% ¹²C) metabolite and the two doublets at 6.74 and 7.09 ppm integrating for 0.2 protons each were assigned to H-3 in the ¹³C₃-enriched metabolite. Thus, approximately 60% of MET-10 was unenriched and ~40% was ¹³C₃-enriched. Assignments were confirmed with a 2D COSY experiment.

To confirm the assignments, a ¹³C NMR experiment (table 5) was

carried out taking advantage of the fact that this metabolite was ¹³C₃-enriched and, therefore, the small amount of isolated metabolite would not be a problem. Carbon assignments were determined with a 2D HMQC experiment. Quaternary carbons were assigned with a 2D HMBC experiment in which the chemical shifts of the protons were correlated to the carbons by means of two-bond and three-bond C-H couplings. The ¹³C NMR assignments for MET-10 indicated the presence of ten carbons. These data together with the ¹H NMR resonances suggested the presence of a carboxylic function in MET-10.

Particle beam EI-MS confirmed this assignment, which showed isotopic molecular ions at m/z 254 and 257 (doublets 3 amu apart owing to the presence of ¹³C₃) corresponding to the addition of a carboxylic acid to the methylsulfonamido indole ring (fig. 5, table 3). Cleavage of CH₃SO₂ gave isotopic fragments at m/z 175 and 178, loss of H₂O gave ions at m/z 157 and 160, with further loss of CO resulting in a fragment at m/z 130. These spectroscopic data identified MET-10 as the indole carboxylic acid metabolite (U-96364). The identity of MET-10 was further confirmed with a synthetic standard, which had identical HPLC retention time as well as a similar EI mass spectrum. However, the ¹H and ¹³C NMR spectra of the synthetic standard were similar to the spectra of MET-10 with few exceptions, which could be explained by the metabolite being a carboxylate salt and the synthetic standard a free carboxylic acid. Assignments were confirmed by addition of triethylamine to the methanol-d₄ solution of U-96364 which resulted in chemical shifts to 6.94 ppm for H-3, 136.2 ppm for C-2, 105.3 ppm for C-3, and 168.4 ppm for the carbonyl carbon.

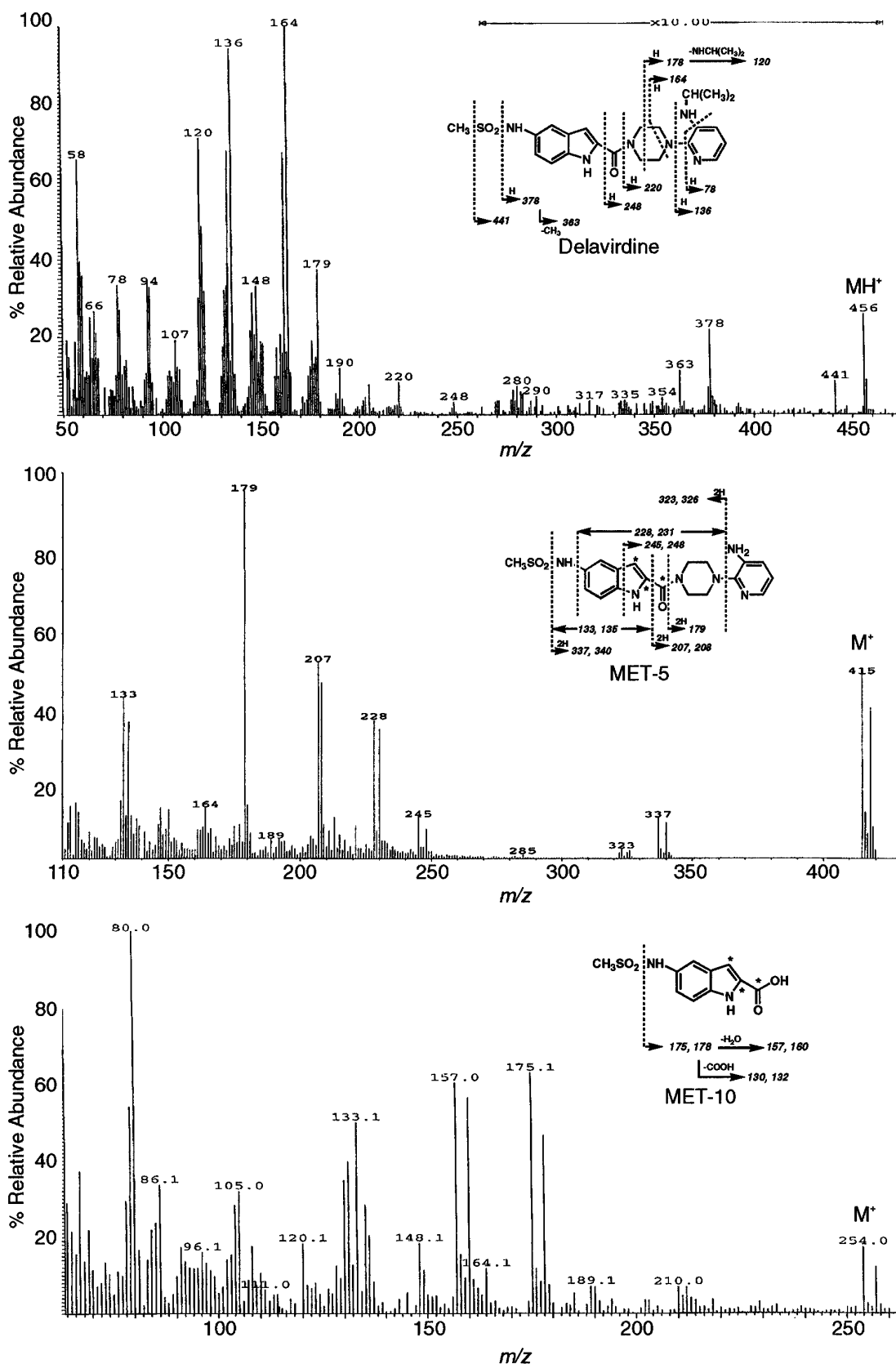


FIG. 5. Mass spectra of delavirdine and its metabolites.

Top to bottom: EI mass spectrum of delavirdine from mouse plasma; CI mass spectrum of MET-5 from mouse urine; EI mass spectrum of MET-10 from mouse urine.

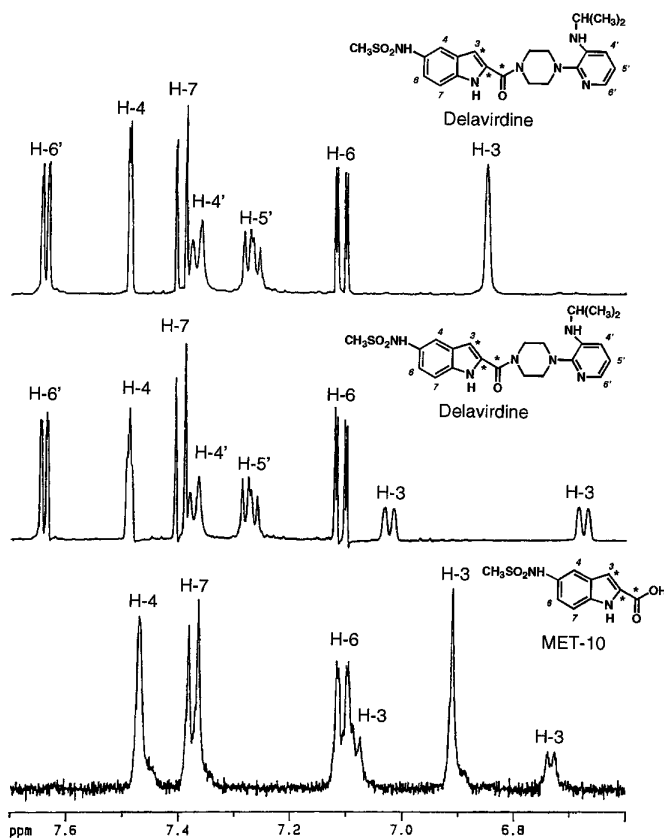


FIG. 6. ^1H NMR spectra (500 MHz) of the aromatic region of delavirdine and its metabolite.

Top to bottom: delavirdine ^{13}C decoupled in $\text{DMSO}-d_6$, delavirdine uncoupled in $\text{DMSO}-d_6$, MET-10 uncoupled in $\text{methanol}-d_4$.

MET-9. MET-9 was observed as a major metabolite in mice after multiple doses of the drug. However, characterization of MET-9 was not possible owing to the instability of this metabolite. A time-course profile of mouse urine indicated that MET-10 was a metabolic precursor of MET-9, most likely a conjugate of U-96364.

Discussion

After oral administration, delavirdine was extensively metabolized before excretion. The major route of excretion was *via* the feces. Excretion of drug-related material was dose dependent; at higher doses and following multiple-dose administration an increased percentage of the administered radioactivity was recovered in urine. Mean urinary excretion in mice ranged from 25–36% of the administered dose and was higher than in rats, where 8–15% of the dose was recovered in urine (27). Gender-related differences in excretion were not observed.

Pharmacokinetic analyses of delavirdine and desalkyl delavirdine in plasma showed that delavirdine was absorbed rapidly with significantly higher concentrations of desalkyl delavirdine than intact delavirdine. The pharmacokinetics of delavirdine were nonlinear, with AUC increasing more than proportionately with dose. The ratio of AUC of desalkyl delavirdine to AUC of delavirdine decreased with increasing dose and suggested that the biotransformation of delavirdine to desalkyl delavirdine was capacity-limited or inhibitable. Desalkyl delavirdine was the major drug-related material in circulation, with parent drug, the thermally labile conjugate of desalkyl delavir-

dine (MET-3), 6'-*O*-glucuronide delavirdine (MET-6), the indole carboxylic acid metabolite (MET-10), and the *N*-isopropylpyridinepiperazine metabolite (MET-12) as minor components. Compared with the rat (27), systemic exposure to delavirdine was significantly lower in the mouse, while systemic exposure to desalkyl delavirdine was significantly higher in the mouse.

Distribution of drug-related radioactivity into mouse brain was low after a 250 mg/kg single-dose of $[2-^{14}\text{C}\text{-pyridine}]$ delavirdine mesylate. In contrast, radioactivity in the pituitary was over 20-fold higher than in the brain 1 hr after dosing. Brain concentrations of delavirdine were <3% of plasma concentrations and indicated that delavirdine did not significantly cross the blood-brain barrier in the mouse. Although concentrations of delavirdine in brain were low (1.9 μM at 1 hr post-dose), these levels exceeded the IC_{50} of 0.26 μM for *in vitro* inhibition of HIV-1 reverse transcriptase by delavirdine (22). In contrast, the *N*-isopropylpyridinepiperazine metabolite readily crossed the blood-brain barrier, with brain concentrations 2- to 3-fold higher than those observed in plasma. The *N*-isopropylpyridinepiperazine metabolite is a D2-dopamine antagonist, and levels of this metabolite have been associated with pseudopregnancy in delavirdine-treated mice (29).

Delavirdine was metabolized by the mouse to several metabolites. Unchanged delavirdine was not detected in urine, indicating extensive metabolism. In urine, desalkyl delavirdine and the indole carboxylic acid or *N*-isopropylpyridinepiperazine metabolites were the major components. These metabolites accounted for 17–27% of the administered dose and were present in roughly equal amounts. At low drug doses, the amounts of desalkyl delavirdine were slightly higher than those of the indole carboxylic acid metabolite, while at high drug doses and after multiple doses the indole carboxylic acid or *N*-isopropylpyridinepiperazine metabolites were present in higher levels than desalkyl delavirdine. These results were consistent with the biotransformation of delavirdine to desalkyl delavirdine reaching saturation or inhibition. In addition, despyridinyl delavirdine (MET-2), the conjugate of the indole carboxylic acid metabolite (MET-9), the thermally labile (MET-3) and sulfate (MET-4a) conjugates of desalkyl delavirdine, 6'-hydroxy delavirdine (MET-7) and its glucuronide conjugate (MET-6), and the *N*-desisopropylpyridinepiperazine metabolite (MET-13, U-91976) were detected as minor components in mouse urine. In contrast, desalkyl delavirdine was the major (5–12% of the dose) drug-related material in rat urine, while MET-10 and MET-12 were very minor metabolites (27). Radioactivity in mouse feces was mostly composed of despyridinyl delavirdine or intact delavirdine after administration of $[^{14}\text{C}\text{-carboxamide}]$ or $[2-^{14}\text{C}\text{-pyridine}]$ delavirdine mesylate, respectively. The differences in metabolite profiles obtained with the carboxamide and pyridine ^{14}C labels and the HPLC analysis of pre-dose feces fortified with $[^{14}\text{C}\text{-carboxamide}]$ delavirdine suggested that bacterial metabolism of delavirdine may account for the presence despyridinyl delavirdine and MET-14 via degradation of 6'-hydroxy delavirdine.

The use of $[^{13}\text{C}_3]$ delavirdine mesylate proved to be indispensable for the identification of metabolites, especially to facilitate interpretation of mass spectra. Fragments containing all three ^{13}C carbons are expected to give doublets 3 amu apart ($A + 3$), while fragments containing two or one ^{13}C carbons would give $A + 2$ or $A + 1$ peaks, respectively, and those with no ^{13}C atoms would yield singlets (see table 3). In addition, ^{13}C NMR spectroscopy of the $^{13}\text{C}_3$ -enriched metabolites could readily be obtained—despite the minute quantities isolated—and this facilitated assignments owing to the presence of one-bond and two-bond carbon-carbon couplings.

TABLE 4

¹H NMR assignments for delavirdine, its metabolite MET-10, and synthetic standard^a

Proton	MET-10 ^b	U-96364 ^b	U-96364 + TEA ^b	[¹³ C ₃]Delavirdine ^c
Indole Ring				
H-3	6.91 ^d (dd, 0.4H, ² J _{C2-H3} = 7.5 Hz, ¹ J _{C3-H3} = 175 Hz) 6.91 (s, 0.6H)	7.12 (s, 1H)	6.94 (s, 1H)	6.86 (dd, 1H, ² J _{C2-H3} = 8 Hz, ¹ J _{C3-H3} = 176 Hz)
H-4	7.47 (d, 1H, J ₄₋₆ = 2.0 Hz)	7.55 (d, 1H, J ₄₋₆ = 2.1 Hz)	7.49 (d, 1H, J ₄₋₆ = 2.1 Hz)	7.49 (d, 1H, J ₄₋₆ = 1.9 Hz)
H-6	7.10 (dd, 1H, J ₆₋₄ = 2.0 Hz, J ₆₋₇ = 8.6 Hz)	7.20 (dd, 1H, J ₆₋₄ = 2.1 Hz, J ₆₋₇ = 8.8 Hz)	7.10 (dd, 1H, J ₆₋₄ = 2.1 Hz, J ₆₋₇ = 8.8 Hz)	7.11 (dd, 1H, J ₆₋₄ = 2.0 Hz, J ₆₋₇ = 8.7 Hz)
H-7	7.37 (d, 1H, J ₇₋₆ = 8.6 Hz)	7.42 (d, 1H, J ₇₋₆ = 8.8 Hz)	7.39 (d, 1H, J ₇₋₆ = 8.8 Hz)	7.40 (d, 1H, J ₇₋₆ = 8.7 Hz)
Pyridine Ring				
H-4'				7.37 (d, 1H, J _{4'-5'} = 8.0 Hz)
H-5'				7.27 (dd, 1H, J _{5'-4'} = 8.0 Hz, J _{5'-6'} = 5.5 Hz)
H-6'				7.64 (dd, 1H, J _{6'-4'} = 1.2 Hz, J _{6'-5'} = 5.5 Hz)
Piperazine Ring				
CH ₂ N				4.02 (br s, 4H)
CH ₂ N				3.30 (br s, 4H)
Isopropyl Chain				
CH				3.70 (m, 1H)
CH ₃				1.20 (d, 6H)
Methylsulfonamido				
CH ₃ SO ₂ NH	2.88 (s, 3H)	2.90 (s, 3H)	2.88 (s, 3H)	2.87 (s, 3H)

^a Abbreviations: br s, broad singlet; d, doublet, dd, doublet of doublets; J, coupling constant in Hz; ¹J, one-bond coupling constant; ²J, 2-bond coupling constant; m, multiplet; s, singlet, t, triplet; TEA, triethylamine.

^b In methanol-d₄, chemical shift δ in ppm relative to methanol.

^c In DMSO-d₆, chemical shift δ in ppm relative to DMSO.

^d Resonance consisted of a doublet at 7.09 ppm integrating for 0.2 protons and another doublet at 6.74 ppm integrating for 0.2 protons.

TABLE 5

¹³C NMR assignments for MET-10 and synthetic standard of U-96364^a

Carbon	MET-10		U-96364	U-96364 + TEA	
	δ	HMQC			HMBC
CO ^b	169.8 (dd, ² J _{CO-C3} = 4.3 Hz, ¹ J _{CO-C2} = 75.4 Hz)	—	—	164.5	168.4
C-2 ^b	137.8 (dd, ¹ J _{C2-C3} = 69.0 Hz, ¹ J _{C2-CO} = 75.5 Hz)	—	6.91	130.5	136.2
C-3 ^b	105.5 (dd, ² J _{C3-CO} = 4.6 Hz, ¹ J _{C3-C2} = 69.0 Hz)	6.91	7.47	108.5	105.3
C-3a	129.3	—	7.37, 6.91	128.5	128.8
C-4	116.9	7.47	—	116.5	116.2
C-5	130.7	—	7.37	131.5	130.5
C-6	120.9	7.10	—	122.5	120.5
C-7	113.4	7.37	—	113.5	112.8
C-7a	135.7	—	6.91, 7.10	136.5	135.2
CH ₃ SO ₂ NH	38.0	2.88	—	38.0	37.8

^a In methanol-d₄, chemical shift δ in ppm relative to methanol.

Abbreviations: dd, doublet of doublets; HMBC, heteronuclear multiple-bond correlation; HMQC, heteronuclear multiple-quantum correlation; ¹J, one-bond coupling constant; ²J, 2-bond coupling constant, TEA, triethylamine.

^b Resonances appeared as doublets of doublets in the spectrum of MET-10 owing to ¹³C-enrichment.

fig. 7 illustrates the scheme for the metabolism of delavirdine in the mouse. The metabolism of delavirdine in the mouse involves four pathways: First, *N*-desalkylation to desalkyl delavirdine (MET-5, U-96183) is followed by conjugation with sulfate (MET-4a) or to MET-3. Second, hydroxylation of delavirdine at the pyridine ring C-6' position to 6'-hydroxy delavirdine (MET-7) and subsequent conjugation with glucuronic acid give 6'-*O*-glucuronide delavirdine (MET-6). Third, the pyridine ring in 6'-hydroxy delavirdine is cleaved to give despyridinyl delavirdine (MET-2, U-102466) and the pyridine ring-opened MET-14. Further conjugation of despyridinyl delavirdine gives MET-1. A fourth pathway involves amide bond cleavage with

release of the *N*-isopropylpyridinepiperazine (MET-12, U-88703) and the indole carboxylic acid (MET-10, U-96364) metabolites and subsequent *N*-desalkylation to the *N*-desisopropylpyridinepiperazine metabolite (MET-13, U-91976) or conjugation of the indole carboxylic acid metabolite to MET-9. Amide bond cleavage represents a major pathway of biotransformation of delavirdine in the mouse, whereas in the rat it is a minor pathway (27).

Acknowledgments. The authors gratefully acknowledge L. R. Norris, R. J. Ouding, K. E. Rousch and T. L. VandeGiessen for technical assistance with animal dosimetry and sample collection. We also

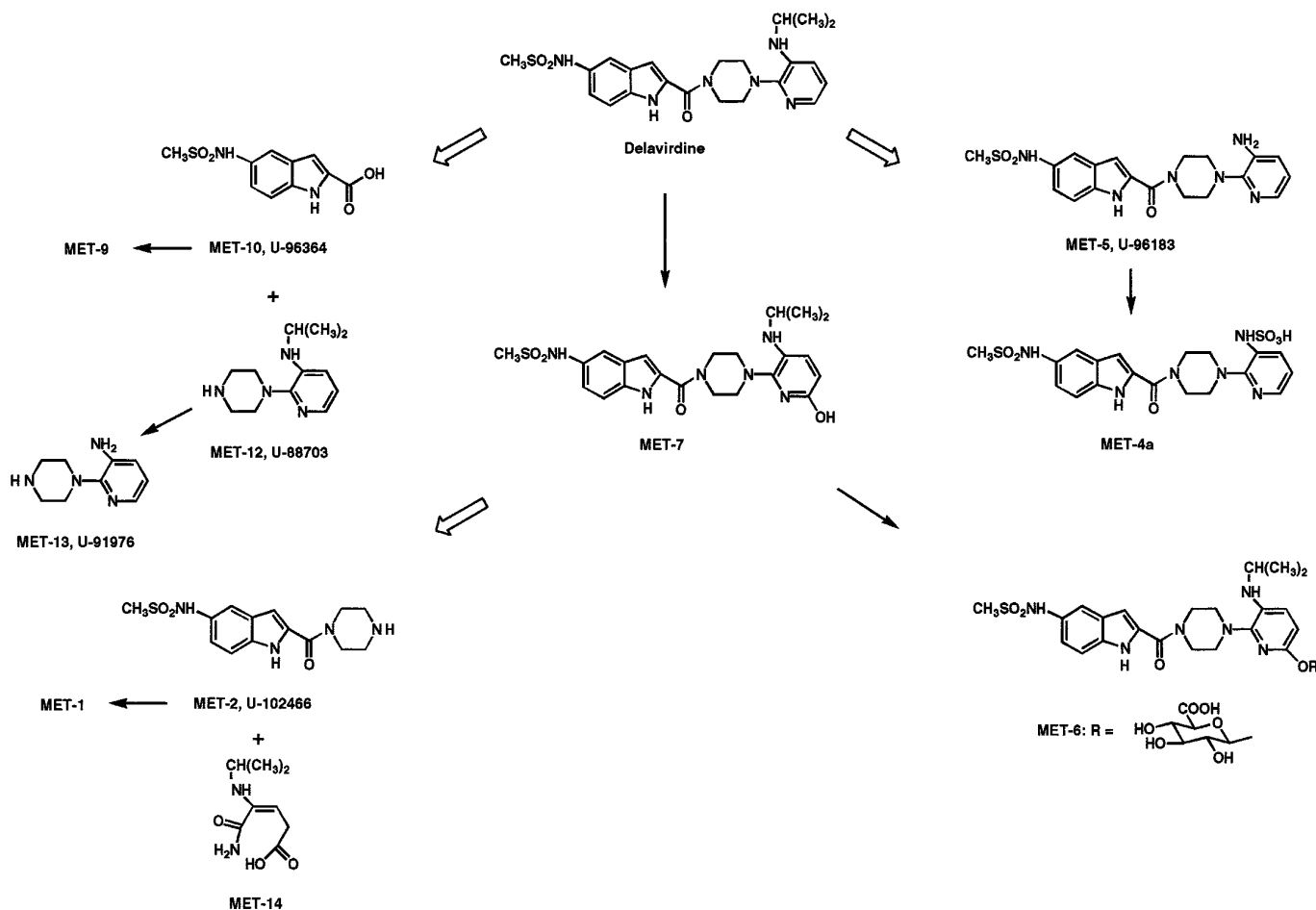


FIG. 7. Metabolic pathway of delavirdine in mice.

thank R. S. P. Hsi, E. H. Chew, W. T. Stolle, and J. A. Easter for syntheses of the ^{14}C and ^{13}C labeled drugs, D. L. Romero for synthesis of U-102466, M. A. Lyster for synthesis of U-91976, and L. J. Larion for preparation of the vehicle in the dosing formulations.

References

- J. S. Mann and D. Tarantola: Coming to terms with the AIDS pandemic. *Issues in Science (Washington DC) and Technology* Spring, 41–48 (1993).
- Y. N. Vaishnav and F. Wong-Staal: The biochemistry of AIDS. *Annu. Rev. Biochem.* **60**, 577–630 (1991).
- H. Mitsuya, R. Yarchoan, and S. Broder: Molecular targets for AIDS therapy. *Science (Washington D. C.)* **249**, 1533–1544 (1990).
- E. De Clercq: Targets and strategies for the antiviral chemotherapy of AIDS. *Trends Pharmacol. Sci.* **11**, 198–205 (1990).
- M. A. Fischl, D. D. Richman, M. H. Grieco, M. S. Gottlieb, P. A. Volberding, O. L. Laskin, J. M. Leedom, J. E. Groopman, D. Mildvan, R. T. Schooley, G. G. Jackson, D. T. Durack, D. King, and The AZT Collaborative Working Group: The efficacy of azidothymidine (AZT) in the treatment of patients with AIDS and AIDS-related complex: a double-blind, placebo-controlled trial. *N. Engl. J. Med.* **317**, 185–191 (1987).
- R. Yarchoan, H. Mitsuya, C. E. Myers, and S. Broder: Clinical pharmacology of 3'-azido-2',3'-dideoxythymidine (zidovudine) and related dideoxynucleosides. *N. Engl. J. Med.* **321**, 726–738 (1989).
- R. Yarchoan, H. Mitsuya, R. V. Thomas, J. M. Pluda, N. R. Hartman, C.-F. Perno, K. S. Marczyk, J. P. Allain, D. G. Johns, and S. Broder: *In vivo* activity against HIV and favorable toxicity profile of 2',3'-dideoxyinosine. *Science (Washington, DC)* **245**, 412–417 (1989).
- J. S. Lambert, M. Seidlin, R. C. Reichman, C. S. Plank, M. Laverty, G. D. Morse, C. Knupp, C. McLaren, C. Pettinelli, F. T. Valentine, and R. Dolin: 2',3'-Dideoxyinosine (ddI) in patients with the acquired immunodeficiency syndrome or AIDS-related complex: a phase I trial. *N. Engl. J. Med.* **322**, 1333–1340 (1990).
- T. P. Cooley, L. M. Kunches, C. A. Saunders, J. K. Ritter, C. J. Perkins, C. McLaren, R. P. McCaffrey, and H. A. Liebman: Once-daily administration of 2', 3'-dideoxyinosine (ddI) in patients with the acquired immunodeficiency syndrome or AIDS-related complex. Results of a phase I trial. *N. Engl. J. Med.* **322**, 1340–1345 (1990).
- R. Yarchoan, R. V. Thomas, J.-P. Allain, N. McAtee, R. Dubinsky, H. Mitsuya, T. J. Lawley, B. Safai, C. E. Myers, C. F. Perno, R. W. Klecker, R. J. Wills, M. A. Fischl, M. C. McNeely, J. M. Pluda, M. Leuther, J. M. Collins, and S. Broder: Phase I studies of 2'-3'dideoxycytidine in severe human immunodeficiency virus infection as a single agent and alternating with zidovudine (AZT). *Lancet* **1**, 76–81 (1988).
- S. A. Riddler, R. E. Anderson, and J. W. Mellors: Antiretroviral activity of stavudine (2',3'-dideoxy-3'-deoxythymidine, d4T). *Antiviral Res.* **27**, 189–203 (1995).
- H. Soudeyns, X.-J. Yao, Q. Gao, B. Belleau, J.-L. Kraus, N. Nguyen-ba, B. Spira, and M. A. Wainberg: Anti-human immunodeficiency virus type 1 activity and *in vitro* toxicity of 2'-deoxy-3'-thiacytidine (BCH-189), a novel heterocyclic nucleoside analog. *Antimicrob. Agents Chemother.* **35**, 1386–1390 (1991).
- J. A. V. Coates, N. Cammack, H. J. Jenkinson, A. J. Jowett, M. I. Jowett, B. A. Pearson, C. R. Penn, P. L. Rouse, K. C. Viner, and J. M. Cameron: (-)-2'-Deoxy-3'-thiacytidine is a potent, highly selective inhibitor of human immunodeficiency virus type 1 and type 2 replication *in vitro*. *Antimicrob. Agents Chemother.* **36**, 733–739 (1992).

14. D. D. Richman, M. A. Fischl, M. H. Grieco, M. S. Gottlieb, P. A. Volberding, O. L. Laskin, J. M. Leedom, J. E. Groopman, D. Mildvan, M. S. Hirsch, G. G. Jackson, D. T. Durack, S. Nusinoff-Lehrman., and The AZT Collaborative Working Group: The toxicity of azidothymidine (AZT) in the treatment of patients with AIDS and AIDS-related complex: A double-blind, placebo-controlled trial. *N. Engl. J. Med.* **317**, 192–197 (1987).
15. H. König, E. Behr, J. Löwer, and R. Kurth: Azidothymidine triphosphate is an inhibitor of both human immunodeficiency virus type I reverse transcriptase and DNA polymerase gamma. *Antimicrob. Agents Chemother.* **33**, 2109–2114 (1989).
16. B. A. Larder and S. D. Kemp: Multiple mutations in HIV-1 reverse transcriptase confer high-level resistance to zidovudine (AZT). *Science (Washington, DC)* **246**, 1155–1158 (1989).
17. B. A. Larder, G. Darby, and D. D. Richman: HIV with reduced sensitivity to zidovudine (AZT) isolated during prolonged therapy. *Science (Washington, DC)* **243**, 1731–1734 (1989).
18. P. Kellam, C. A. B. Boucher, and B. A. Larder: Fifth mutation in a human immunodeficiency virus type I reverse transcriptase contributes to the development of high-level resistance to zidovudine. *Proc. Natl. Acad. Sci. USA* **89**, 1934–1938 (1992).
19. M. H. St. Clair, J. L. Martin, G. Tudor-Williams, M. C. Bach, C. L. Vavro, D. M. King, P. Kellam, S. D. Kemp, and B. A. Larder: Resistance to ddi and sensitivity to AZT induced by a mutation in HIV-1 reverse transcriptase. *Science (Washington, DC)* **253**, 1557–1559 (1991).
20. R. Schuurman, M. Nijhuis, R. van Leeuwen, P. Schipper, D. de Jong, P. Collis, S. A. Danner, J. Mulder, C. Loveday, C. Christopherson, S. Kwok, J. Sninsky, and C. A. B. Boucher: Rapid changes in human immunodeficiency virus type 1 RNA load and appearance of drug-resistant virus populations in persons treated with lamivudine (3TC). *J. Infect. Dis.* **17**, 1411–1419 (1995).
21. T. J. Dueweke, S. M. Poppe, D. L. Romero, S. M. Swaney, A. G. So, K. M. Downey, I. W. Althaus, F. Reusser, M. Busso, L. Resnick, D. Mayers, J. Lane, P. A. Aristoff, R. C. Thomas, and W. G. Tarpley: U-90152, a potent inhibitor of human immunodeficiency virus type 1 replication. *Antimicrob. Agents Chemother.* **37**, 1127–1131 (1993).
22. D. L. Romero, R. A. Morge, M. J. Genin, C. Biles, M. Busso, L. Resnick, I. W. Althaus, F. Reusser, R. C. Thomas, and W. G. Tarpley: Bis(heteroaryl)piperazine (BHAP): reverse transcriptase inhibitors: Structure-activity relationships of novel substituted indole analogues and the identification of 1-[(5-methanesulfonamido-1H-indol-2-yl)-carbonyl]-4-[3-[(1-methylethyl)amino]-pyridinyl]piperazine monomethanesulfonate (U-90152S), a second-generation clinical candidate. *J. Med. Chem.* **36**, 1505–1508 (1993).
23. A. Bax, R. H. Griffey, and B. L. Hawkins: Correlation of proton and nitrogen-15 chemical shifts by multiple quantum NMR. *J. Magn. Reson.* **55**, 301–315 (1983).
24. A. Bax and M. F. Summers: Proton and carbon-13 assignments from sensitivity-enhanced detection of heteronuclear multiple-bond connectivity by 2D multiple quantum NMR. *J. Am. Chem. Soc.* **108**, 2093–2094 (1986).
25. A. J. Shaka, P. B. Barker, and R. Freeman: Computer-optimized decoupling scheme for wideband applications and low-level operation. *J. Magn. Reson.* **64**, 547–552 (1985).
26. D. M. Doddrell, D. T. Pegg, and M. R. Bendall: Distortionless enhancement of NMR signals by polarization transfer. *J. Magn. Reson.* **64**, 547–552 (1985).
27. M. Chang, V. K. Sood, G. J. Wilson, D. A. Kloosterman, P. E. Sanders, M. J. Hauer, and P. E. Fagerness: Metabolism of the reverse transcriptase inhibitor delavirdine in rats. *Drug Metab. Dispos.* **25**, 228–242 (1997).
28. V. K. Sood, D. A. Kloosterman, P. E. Sanders, M. J. Hauer, J. J. Vrbanac, and M. Chang: Metabolism of the reverse transcriptase inhibitor delavirdine: Identification of novel *N*-acetylglucosamine and pyridinol sulfate conjugates. Presented at “Fourth International Meeting of the International Society for the Study of Xenobiotics,” (Abstract), Seattle, 1995.
29. V. K. Sood, W. Zhang, D. G. Branstetter, and M. Chang: Mechanism of delavirdine-induced pseudopregnancy in mice. Presented at “Seventh North American Meeting of the International Society for the Study of Xenobiotics,” (Abstract), San Diego, 1996.